Engineering Computations

Convergence behavior of 3D finite elements for Neo-Hookean material

Erwin Stein, Gautam Sagar,

Article information:

Received 15 May 2007
Revised 7 November 2007
Accepted 8 November 2007

Convergence behavior of 3D finite elements for Neo-Hookean material

Erwin Stein and Gautam Sagar
Institute of Mechanics and Computational Mechanics, Leibniz University of Hannover, Hannover, Germany

Abstract

Purpose – The purpose of this paper is to examine quadratic convergence of finite element analysis for hyperelastic material at finite strains via Abaqus-UMAT as well as classification of the rates of convergence for iterative solutions in regular cases.

Design/methodology/approach – Different formulations for stiffness – Hessian form of the free energy functionals – are systematically given for getting the rate-independent analytical tangent and the numerical tangent as well as rate-dependent tangents using the objective Jaumann rate of Kirchoff stress tensor as used in Abaqus. The convergence rates for available element types in Abaqus are computed and compared for simple but significant nonlinear elastic problems, such as using the 8-node linear brick (B-bar) element – also with hybrid pressure formulation and with incompatible modes – further the 20-node quadratic brick element with corresponding modifications as well as the 6-node linear triangular prism element and 4-node linear tetrahedral element with modifications.

Findings – By using the Jaumann rate of Kirchoff stress tensor for both, rate dependent and rate independent problems, quadratic or nearly quadratic convergence is achieved for most of the used elements using Abaqus-UMAT interface. But in case of using rate independent analytical tangent for rate independent problems, even convergence at all is not assured for all elements and the considered problems.

Originality/value – First time the convergence properties of 3D finite elements available in Abaqus sre systematically treated for elastic material at finite strain via Abaqus-UMAT.

Keywords Finite element analysis, Alloys, Kinematics

Paper type Research paper

Introduction

Abaqus standard provides the user interface UMAT for the implementation of user defined material equations. The user can take advantage of the complete finite element program from Abaqus and has to focus on the material model. To implement finite strain kinematics for hyperelastic materials in a finite element program one likes to have an efficient tangent which provides quadratic convergence in regular cases of solids and structural mechanics (elliptical problems). Mainly two types of tangents are available, the analytical material tangent (stiffness matrix) in each point of a chosen continuous configuration and the consistent (numerical) tangent, defined in each Gaussian integration point of the finite element discretization, which has to be provided by the user.

The authors would like to thank Professor Jörg Schröder, Universität Duisburg-Essen, for discussion. Support for this work is provided by the German Science Foundation (DFG) under project No. Ste 238/51-1, which is gratefully acknowledged.

Engineering Computations: International Journal for Computer-Aided Engineering and Software
Vol. 25 No. 3, 2008
pp. 220-232

0264-4401
DOI 10.1108/02644400810857065

This paper was written in parallel to the development of finite strain theory and analysis of martensitic phase transformation (PT) in metal alloys (Stein and Sagar, 2007), using the UMAT-interface with C + + where severe problems arose. The treatment of small deformation PT is given in Stein and Zwickert (2007).

For Abaqus UMAT interface it is necessary to use Jaumann rate of Kirchoff stress tensor as a tangent in current configuration, for both rate dependent and rate independent problems in case of nonlinear deformation processes.

The first two sections advocate results from finite strain continum mechanics which are widely known. Therefore, the presentation is as short as possible to derive the essential features in the section for tangent moduli.

Analytical tangent

Kinematics

The kinematics of solid bodies are characterized by two different motions: rigid body displacement and rotation as well as deformation. The deformations of a body can be described by mapping operators and geometrical quantities. In Figure 1 on the left, an undeformed solid body $\mathscr{B}_0$ – which defines the initial stress free reference configuration – is shown; it is used as reference configuration. The deformed configuration $\mathscr{B}_t$ is called as actual or current configuration. The quantities related to reference configuration are written in capital letters and quantities related to current configuration are written in small letters.

In a material setting the displacement vector of point $\mathbf{X}$ of body $\mathscr{B}_0$ is denoted as $\mathbf{u}_t = x_t(\mathbf{X}, t, t_0) - \mathbf{X}(t_0)$.

Deformation in material description

The non-symmetric material deformation gradient, $\mathbf{F}(\mathbf{X}, t, t_0) := \text{grad}\varphi(\mathbf{X}, t, t_0)$, $\mathbf{J} := \det \mathbf{F} \neq 0$ defines a tangential (linear) mapping. It maps the infinitesimal material vector $\mathrm{d}\mathbf{X}$ into an infinitesimal vector, $\mathrm{d}\mathbf{x} = \mathbf{F}\,\mathrm{d}\mathbf{X}$. The material deformation gradient can also be written symbolically as, $\mathbf{F} = \mathrm{d}\mathbf{x}/\mathrm{d}\mathbf{X} = 1 + \nabla\mathbf{u}(\mathbf{X}, t, t_0)$, with $\mathbf{H}(\mathbf{X}) := \nabla\mathbf{u}(\mathbf{X})$ the material displacement gradient. $\mathbf{F}$ can be split into a stretch tensor $\mathbf{U}$ and a true orthogonal rotation tensor $\mathbf{R}$ as $\mathbf{F} = \mathbf{R}\,\mathbf{U}$ with $\mathbf{R}^{\mathrm{T}} = \mathbf{R}^{-1}$; det$\mathbf{R}$ and $\mathbf{U} = \mathbf{U}^{\mathrm{T}}$.

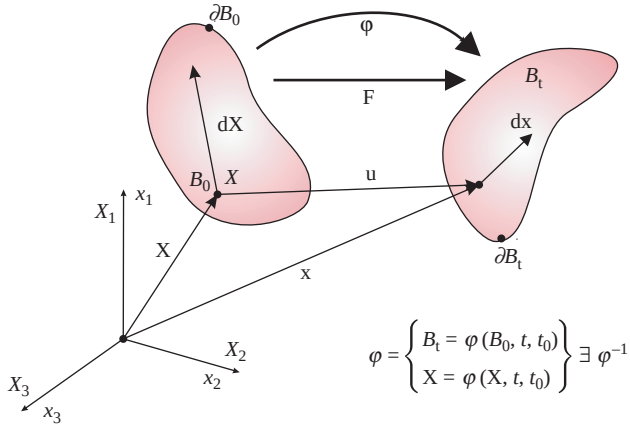

Figure 1.
Initial configuration $\mathscr{B}_0$ and actual configuration $\mathscr{B}_t$ of a solid body connected by a bijective non-linear mapping ϕ and the tangent mapping $\mathbf{F}$

Deformation in spatial description

The spatial velocity gradient $\mathbf{l}$ follows from $\mathrm{d}\dot{\mathbf{X}} = \mathbf{l} \cdot \mathrm{d}\dot{\mathbf{x}}$ and reads:

$$\mathbf{l} = \dot{\mathbf{F}} \cdot \mathbf{F}^{-1} \tag{1}$$

$$\text{with } \mathbf{l} := \mathrm{grad}\mathbf{v}(\mathbf{x}) = \mathrm{grad}(\dot{\mathbf{x}}) = \mathbf{d} + \mathbf{w}, \tag{2}$$

$$\text{where } d = \mathrm{grad}_{\mathrm{sym.}}\mathbf{v}(\mathbf{x}) \text{ and } \mathbf{w} = \mathrm{grad}_{\mathrm{skew}}\mathbf{v}(\mathbf{x}). \tag{3}$$

Stiffness derived from an energy function

The second Piola-Kirchhoff (PK) stress tensor is derived from the free energy function ψ in the case of hyperelastic material as, see, e.g. Wriggers (2001):

$$\mathbf{S} = 2\frac{\partial \psi(\mathbf{C})}{\partial \mathbf{C}}, \tag{4}$$

with $\mathbf{C} = \mathbf{F}^{\mathrm{T}}\mathbf{F}$ the right Cauchy-Green deformation tensor, $\mathbf{C} = \mathbf{C}^{\mathrm{T}}$, $\det\mathbf{C} > 0$ and $\sqrt{\mathbf{C}} = \mathbf{U}$.

The strain energy function can be specialized and is represented here by an isotropic tensor function:

$$\psi(\mathbf{C}) = \psi(\mathrm{I}_{\mathbf{C}}, \mathrm{II}_{\mathbf{C}}, \mathrm{III}_{\mathbf{C}}), \tag{5}$$

where $\mathrm{I}_{\mathbf{C}}$, $\mathrm{II}_{\mathbf{C}}$ and $\mathrm{III}_{\mathbf{C}}$ are 1st, 2nd, and 3rd invariants of $\mathbf{C}$. The second PK stress follows from equation (4) can be transformed directly into the current (spatial) configuration by the standard push forward operation yielding the Kirchhoff stress tensor $\boldsymbol{\tau} = \mathbf{F}\,\mathbf{S}\,\mathbf{F}^{\mathrm{T}}$ with $\boldsymbol{\tau} = \mathbf{J}\boldsymbol{\sigma}$ where $\boldsymbol{\sigma}$ is the Cauchy stress tensor.

Kirchhoff stress tensor in terms of spatial quantities for isotropic materials (Miehe, 1996) reads:

$$\boldsymbol{\tau} = 2\mathbf{b} \cdot \frac{\partial \psi(\mathbf{b})}{\partial \mathbf{b}}. \tag{6}$$

The incremental elasticity tensor $\mathbf{C}(\mathbf{E})$ in the reference configuration is defined for a hyperelastic material via the Green strain tensor $\mathrm{d}\mathbf{S} = \mathbb{C}(\mathbf{E}) : \mathrm{d}\mathbf{E}$ with $\mathbf{E} := 1/2(\mathbf{F}^{\mathrm{T}} \cdot \mathbf{F} - 1)$ and is the Hessian of the free energy function $\mathbb{C}(\mathbf{E}) = \partial^2\psi(\mathbf{C})/\partial\mathbf{E}\partial\mathbf{E}$. This can be transformed directly into $c(\mathbf{b})$ in spatial coordinate by the standard push forward operation. The tangential spatial elasticity tensor for the Kirchhoff stress (Miehe, 1996) then reads:

$$\mathbf{c}^{\tau}(b) = 4\mathbf{b} \cdot \frac{\partial^2 \psi(\mathbf{b})}{\partial \mathbf{b} \partial \mathbf{b}} \cdot \mathbf{b}. \tag{7}$$

Numerical tangent

In the Abaqus 6.4 documentation (Abaqus, n.d.) the variation of the symmetric spatial rate of deformation tensor is defined as:

$$\delta\mathbf{D} \equiv \delta\mathbf{d} = \dot{\varepsilon}\delta t, \quad \text{where } \delta t \text{ is the linearized time increment,} \tag{8}$$

with the symmetric spatial rate of deformation tensor:

$$\delta\mathbf{d} = \mathrm{sym}\delta\mathbf{l} = \mathrm{sym}\delta(\dot{\mathbf{F}} \cdot \mathbf{F}^{-1}) \tag{9}$$

$$= \mathrm{sym}(\mathrm{grad}\dot{\mathbf{x}}) \cdot \delta t \tag{10}$$

and the linear strain rate measure used in Abaqus $\dot{\boldsymbol{\varepsilon}} := \mathrm{sym}(\mathrm{grad}\dot{\mathbf{x}})$.

The Jaumann rate of the left Cauchy-Green tensor, $\mathbf{b} = \mathbf{F}\,\mathbf{F}^{\mathrm{T}}$, follows as:

$$\overset{\nabla}{\mathbf{b}} = \mathbf{d}\cdot\mathbf{b} + \mathbf{b}\cdot\mathbf{d}. \tag{11}$$

The linear increment of $\mathbf{b}$ is:

$$\mathrm{d}\mathbf{b} = \overset{\nabla}{\mathbf{b}}\cdot\mathrm{d}t = (\mathbf{d}\cdot\mathbf{b} + \mathbf{b}\cdot\mathbf{d})\cdot\mathrm{d}t \tag{12}$$

$$= (\mathrm{d}\boldsymbol{\varepsilon}\cdot\mathbf{b} + \mathbf{b}\cdot\mathrm{d}\boldsymbol{\varepsilon}), \tag{13}$$

or in index notation, see also (Besdo *et al.*, 2005):

$$\delta b^{ab} = \delta\varepsilon^{ac} b^{cb} + b^{ac}\delta\varepsilon^{cb} \quad \text{with } a,b = 1,2,3. \tag{14}$$

Separate representation of virtual left Cauchy-Green deformation and superposition for the virtual strain rate component $\delta\varepsilon^{11} \equiv \delta\varepsilon$ yields:

$$\delta\mathbf{b}_{1^{\circledast}}^{(\delta\varepsilon_{11})} = \begin{bmatrix} \delta\varepsilon & 0 & 0 \\ 0 & 0 & 0 \\ 0 & 0 & 0 \end{bmatrix} \begin{bmatrix} b^{11} & b^{12} & b^{13} \\ b^{12} & b^{22} & b^{23} \\ b^{13} & b^{23} & b^{33} \end{bmatrix} + \begin{bmatrix} b^{11} & b^{12} & b^{13} \\ b^{12} & b^{22} & b^{23} \\ b^{13} & b^{23} & b^{33} \end{bmatrix} \begin{bmatrix} \delta\varepsilon & 0 & 0 \\ 0 & 0 & 0 \\ 0 & 0 & 0 \end{bmatrix} \tag{15}$$

$$= \delta\varepsilon \begin{bmatrix} b^{11} & b^{12} & b^{13} \\ 0 & 0 & 0 \\ 0 & 0 & 0 \end{bmatrix} + \begin{bmatrix} b^{11} & 0 & 0 \\ b^{12} & 0 & 0 \\ b^{13} & 0 & 0 \end{bmatrix} \delta\varepsilon \tag{16}$$

$$= \delta\varepsilon \begin{bmatrix} 2b^{11} & b^{12} & b^{13} \\ b^{12} & 0 & 0 \\ b^{13} & 0 & 0 \end{bmatrix} = \delta\varepsilon\mathbf{b}_{1^{\circledast}} \tag{17}$$

and $b^{12} = b^{21}$ for shear deformation.

In total, six separate representations for $\delta\varepsilon^{11}$, $\delta\varepsilon^{22}$, $\delta\varepsilon^{33}$, $\delta\varepsilon^{12} = \delta\varepsilon^{21}$, $\delta\varepsilon^{23} = \delta\varepsilon^{32}$, $\delta\varepsilon^{13} = \delta\varepsilon^{31}$, $[\delta\varepsilon] = 1$, have to be regarded, together:

$$\delta\mathbf{b} = \delta\varepsilon \sum_{i^{\circledast}=1}^{6} \mathbf{b}_{i^{\circledast}}. \tag{18}$$

Defining positive and negative changes of $\mathbf{b}$ and $\boldsymbol{\sigma}$ through their variations:

$$\mathbf{b}^{+} := \mathbf{b} + \delta\mathbf{b}; \quad \mathbf{b}^{-} = \mathbf{b} - \delta\mathbf{b} \text{ and} \tag{19}$$

$$\boldsymbol{\sigma}^{+} := f(\mathbf{b}^{+}, J^{+}); \quad \boldsymbol{\sigma}^{-} := f(\mathbf{b}^{-}, J^{-}), \tag{20}$$

the variation of $\mathbf{b}$ can be expressed as:

$$\delta\mathbf{b} = -\mathbf{b} + \mathbf{b}^{+} = \mathbf{b} - \mathbf{b}^{-} \tag{21}$$

$$2\delta\mathbf{b} = -\mathbf{b} + \mathbf{b}^{+} + \mathbf{b} - \mathbf{b}^{-} = \mathbf{b}^{+} - \mathbf{b}^{-} \tag{22}$$

$$\delta\mathbf{b} = \frac{\mathbf{b}^{+} - \mathbf{b}^{-}}{2}; (\text{mid point rule}). \tag{23}$$

Equation (18) in inserted into equation (23) yields the variation:

$$\delta\mathbf{b} = \delta\varepsilon \sum_{i^{\circledast}=1}^{6} \frac{\mathbf{b}_{i^{\circledast}}^{+} - \mathbf{b}_{i^{\circledast}}^{-}}{2}. \tag{24}$$

Similar to equation (24) the incremental Cauchy stress follows as:

$$\delta\boldsymbol{\sigma} = \delta\varepsilon \sum_{i^{\circledast}=1}^{6} \frac{\boldsymbol{\sigma}_{i^{\circledast}}^{+} - \boldsymbol{\sigma}_{i^{\circledast}}^{-}}{2}. \tag{25}$$

The stiffness related to Cauchy stress then reads:

$$\mathrm{c} = \begin{Bmatrix} \frac{\delta\boldsymbol{\sigma}_{1^{\circledast}}}{\delta\varepsilon} \\ \cdot \\ \cdot \\ \frac{\delta\boldsymbol{\sigma}_{i^{\circledast}}}{\delta\varepsilon} \\ \cdot \\ \frac{\delta\boldsymbol{\sigma}_{6^{\circledast}}}{\delta\varepsilon} \end{Bmatrix}. \tag{26}$$

Jaumann rate formulation for tangent moduli

The objective Lie derivative, see, e.g. Simo and Hughes (1998) and de Bore and Schröder (2007), of the Kirchhoff stress tensor is got as the push forward operation of the time derivative of **S:**

$$\mathscr{L}_V\boldsymbol{\tau} := \mathbf{F}\left\{\frac{\partial}{\partial t}\left[\mathbf{F}^{-1}\cdot\boldsymbol{\tau}\cdot\mathbf{F}^{-\mathrm{T}}\right]\right\}\cdot\mathbf{F}^{\mathrm{T}} = \mathbf{F}\cdot\left\{\frac{\partial}{\partial t}\left[\mathbf{S}\right]\right\}\cdot\mathbf{F}^{\mathrm{T}}, \tag{27}$$

with the 2-PK stress tensor $\mathbf{S} := \mathbf{F}^{-1}\mathbf{P}$; $\mathbf{P}$ the $1-\mathbf{PK}$ stress and the time derivative of $\mathbf{F}^{-1}$:

$$\frac{\partial}{\partial t}(\mathbf{F}^{-1}) = -\mathbf{F}^{-1}\cdot\frac{\partial\mathbf{F}}{\partial t}\cdot\mathbf{F}^{-1}. \tag{28}$$

The Lie derivative by using equation (2) reads:

$$\mathscr{L}_V\boldsymbol{\tau} = \dot{\boldsymbol{\tau}} - \mathbf{l}\cdot\boldsymbol{\tau} - \boldsymbol{\tau}\cdot\mathbf{l}^{\mathrm{T}}. \tag{29}$$

The Abaqus user interface UMAT requires a tangent (stiffness) which is associated with the Jaumann rate of the Cauchy stress. The Jaumann rate of the Kirchhoff stress $\overset{\nabla}{\boldsymbol{\tau}}$ is the corotated objective time derivative with respect to the spatial configuration with instantaneous velocity $\mathbf{v}(\mathbf{x})$, given by the skew symmetric (spin) tensor $\mathbf{w}$ (i.e. the vorticity).

$$\overset{\nabla}{\boldsymbol{\tau}} := \dot{\boldsymbol{\tau}} - \mathbf{w}\cdot\boldsymbol{\tau} - \boldsymbol{\tau}\cdot\mathbf{w}^{\mathrm{T}}. \tag{30}$$

By using equations (29) and (30), we get a relation between the Jaumann stress rate and the Lie derivative of the Kirchoff stress in spatial coordinates:

$$\overset{\nabla}{\boldsymbol{\tau}} := \mathscr{L}_V\boldsymbol{\tau} + \mathbf{d}\cdot\boldsymbol{\tau} + \boldsymbol{\tau}\cdot\mathbf{d}^{\mathrm{T}}. \tag{31}$$

With the spatial tangent matrix $\mathbf{c}$, the Lie derivative of the Kirchoff stress can be written as:

$$\mathscr{L}_V\boldsymbol{\tau} = \mathbf{c} : \mathbf{d} \;\text{ or }\; (\mathscr{L}_V\boldsymbol{\tau})^{ab} = \mathbf{c}^{abcd} : \mathbf{d}^{cd}. \tag{32}$$

From equations (31) and (32) we get the Jaumann rate of the Kirchoff stress associated with $\overset{\nabla}{\mathbf{c}}$ as the Jaumann rate of $\mathbf{c}$ in the form:

$$\overset{\nabla}{\boldsymbol{\tau}} = \overset{\nabla}{\mathbf{c}} : \mathbf{d} \;\text{ or }\; (\overset{\nabla}{\boldsymbol{\tau}})^{ab} = (\overset{\nabla}{\mathbf{c}})^{abcd} : \mathbf{d}^{cd}. \tag{33}$$

In index notation this takes the form, see, e.g. Simo and Hughes (1998):

$$(\overset{\nabla}{\mathbf{c}})^{abcd} = \mathbf{c}^{abcd} + \delta^{ac}\boldsymbol{\tau}^{bd} + \boldsymbol{\tau}^{ac}\delta^{bd}. \tag{34}$$

$(\delta^{ac}\boldsymbol{\tau}^{bd} + \boldsymbol{\tau}^{ac}\delta^{bd})$ is lacking minor symmetry and by making it symmetric reads:

$$(\overset{\nabla}{\mathbf{c}})^{abcd} = \mathbf{c}^{abcd} + \frac{1}{2}(\delta^{ac}\boldsymbol{\tau}^{bd} + \boldsymbol{\tau}^{ac}\delta^{bd} + \delta^{ad}\boldsymbol{\tau}^{bc} + \boldsymbol{\tau}^{ad}\delta^{bc}). \tag{35}$$

For the user subroutine UMAT the Cauchy stress is required which is derived from $\boldsymbol{\tau}$ as $\boldsymbol{\sigma} = \tau/\mathbf{J}$ and the tangent, $\tilde{\mathbf{c}}$, related to Jaumann rate of Kirchoff stress tensor (for Abaqus) reads:

$$\tilde{\mathbf{c}}^{abcd} := \overset{\nabla}{\mathbf{c}}{}^{abcd}/\mathbf{J} = [\mathbf{c}^{abcd} + (1/2(\delta^{ac}\boldsymbol{\tau}^{bd} + \boldsymbol{\tau}^{ac}\delta^{bd} + \delta^{ad}\boldsymbol{\tau}^{bc} + \boldsymbol{\tau}^{ad}\delta^{bc}))]/\mathbf{J} \tag{36}$$

where $\mathbf{c}^{abcd}$ is the spatial tangent which is equivalent to $\mathbf{c}^{\boldsymbol{\tau}}(\mathbf{b})$, equation (7).

To implement a nonlinear material model (related to finite strain kinematics) in Abaqus via user subroutine UMAT the required tangent (stiffness) is expressed by equation (36).

Implementation of a Neo-Hookean material model in Abaqus 6.4 via UMAT

The algorithms for the nonlinear material law are converted into the C++ programming language and coupled by Abqus via UMAT. Figure 2 shows the flow chart for interaction of subroutine. At the beginning of each (process) time step UMAT is called for every integration point of the finite elements in Abaqus. DFGRD1 (deformation gradient at the end of increment) delivered from Abaqus gives the information for deformation gradient and is used for material subroutine. The new stress (STRESS), equation (6), and the material tangent (DDSDDE) following from equation (36) are calculated. At the end of UMAT the new values are allocated to the variables STRESS and DDSDDE.

Before the declaration of the C++ subroutine the expression "extern 'C' " has to appear. For using a "character string" which is passed from FORTRAN to the C++ routine one has to implement a function that converts a FORTRAN CHARACTER string into a C++ string which are not compatible. In order to reach compatibility functions callable for FORTRAN must be declared as:

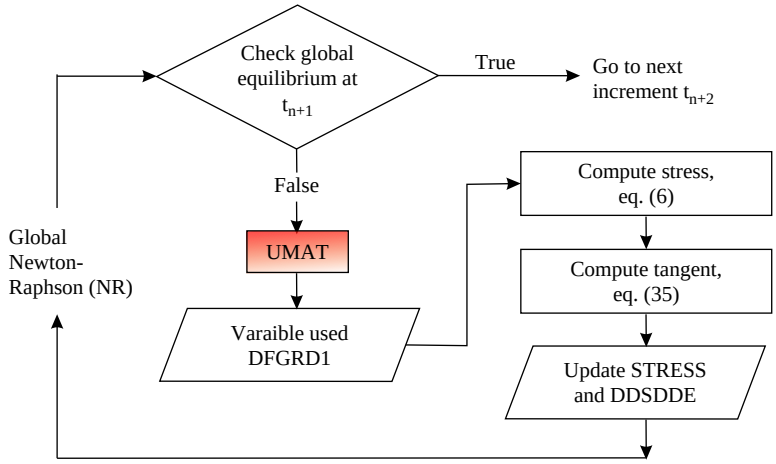

Figure 2.
Flow chart for the interaction of Abaqus and UMAT

...FOR_NAME(subnam,SUBNAM) (...).

The FOR_NAME macro allows system-dependent handling of function names.

Depending on the Abaqus version (we used version 6.4) and the installed compilers the UMAT subroutine has to be compiled by a command contained in the data file abaqus_X.env (with version number X) located in the Abaqus installation directory under...\Version\site.

For the version 6.4 and the compilers Visual C++6.0 and Visual Fortran 6 the UMAT has to be compiled with:

"cl/c/nologo/W0/MD/TP/DNDEBUG/DWIN32/DTP_IP/D_CONSOLE/DNTI/DFLT_LIC/DOL_DOC/D__LIB__/DHKS_NT/DFAR = /D_WINDOWS/O1/Iper centI".

First material model

The total strain energy ψ of two parameter model, see, e.g. Wriggers (2001), results as:

$$\psi(I_c, J) = g(J) + \frac{1}{2}\mu(I_c - 3), \tag{37}$$

$$\text{with } g(J) = c(J^2 - 1) - d\ln J - \mu \ln J, \tag{38}$$

$$I_c = \text{trace}(\mathbf{C}), \quad c = \Lambda/4, \quad d = \Lambda/2 \tag{39}$$

$$\mathbf{C} := \mathbf{F}^{\mathrm{T}} \cdot \mathbf{F}, \quad \text{the right Cauchy} - \text{Green tensor}, \tag{40}$$

with c>0, d>0. Λ and μ are Lamé parameters where μ is the shear modulus.

The Cauchy stress is obtained as:

$$\boldsymbol{\sigma} = 2\mathbf{J}^{-1}\mathbf{F}\frac{\delta\psi}{\delta\mathbf{C}}\mathbf{F}^{\mathrm{T}} = \frac{\Lambda}{2}(\mathbf{J}^2 - 1)\mathbf{I} + \frac{\mu}{J}(\mathbf{b} - \mathbf{I}). \tag{41}$$

The tangent in the current configuration results in, see, e.g. Wriggers (2001):

$$\mathbf{c}^{abcd} = \Lambda J^2 \delta^{ab}\delta^{cd} + \left[2\mu - \Lambda(J^2 - 1)\right]\mathbb{I}^{abcd}, \tag{42}$$

with the components of the fourth order unity tensor:

$$\mathbb{I}^{abcd} = \frac{1}{2}(\delta^{ac}\delta^{bd} + \delta^{ad}\delta^{bc}). \tag{43}$$

$\mathbf{c}_{abcd}$ in equation (42) is equal to $\mathbf{c}^{abcd}$ in equation (36). By using equations (36), (42) and (43) we get the tangent for Abaqus UMAT interface (Figure 3).

Examples

The analytical tangent, equation (42) with the modification ($J^{-1}\mathbf{c}^{abcd}$), numerical tangent, equation (26) and objective Jaumann rate of Kirchhoff stress for rate dependent deformation, equation (36), are implemented in Abaqus via UMAT interface. The computed results from different tangents (siffnesses) are computed for different:

- mesh sizes;
- element types;
- displacement controls; and
- maximum number of displacement increments.

The finite element computations were performed for 13 cases with comparative studies. The goal of this is the classification of the rates of convergence for iterative solutions in regular cases, especially the intended quadratic convergence of appropriate iterative solvers for nonlinear algebraic equations. The default value of convergence tolerance is taken from Abaqus. This tolerance parameter for residual force of investigated problems is 5.000E-03.

A cube with edges of unit length l is chosen for the following examples, Figure 2. The left face, ABCD of the cube is constrained in X direction (as direction 1), the bottom face, ADHE of the cube is constrained in the Y direction (as direction 2) and the back face, ABFE is constrained in Z direction (as direction 3). Displacements are applied at the corner G ($X = Y = Z = l$). The material parameters are obtained from the chosen Young's modulus, $E = 7$ MPa, and Poisson's ratio, $\nu = 0.4999$, for the computations.

It is found that the numerical tangent, equation (26), and the analytical tangent obtained from $\mathrm{J}^{-1}\mathbf{c}^{abcd}$, equation (7), are not at all efficient. Either the convergence

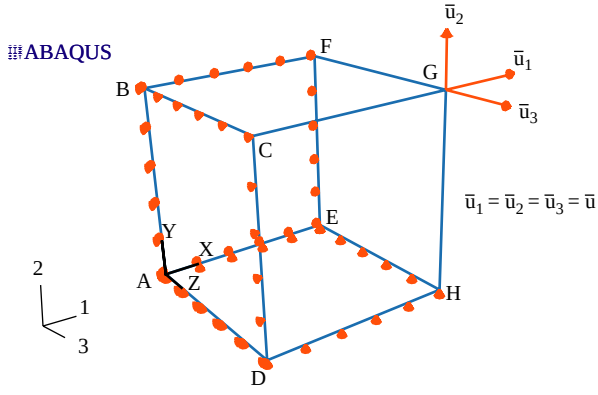

Figure 3.
Unit cube in reference configuration with boundary conditions and applied loads

rates are not quadratic or the related equation systems even do not converge. The stiffness is obtained by Jaumann rate of Kirchhoff stress tensor, equation (36), for UMAT interface and results are presented (Table I).

Element C3D8

An 8-node linear brick (hexahedral) B-bar element is used.

No. of elements: $5 \times 5 \times 5$, displacements, $u_x = u_y = u_z = 0.5$, increment type: fixed, and maximum number of increments: 25 (Table II).

Results and discussion.

- *Number of iterations*. Two iterations are needed for each increment.
- *Convergence rate*. The convergence rate is quadratic.

Element C3D4

It is a 4-node linear tetrahedral element. No. of seeds (nodes): $5 \times 5 \times 5$ (five seeds in each direction), displacements, $u_x = u_y = u_z = 0.5$, increment type: fixed, and maximum number of increments: 25.

Results and discussion. Number of iterations and increments.

Increment No.	1	2	3	4	5	6	7	8	9	10	11	12	13	14
No. of iterations	3	3	3	3	3	2	2	2	2	2	2	2	2	2

Increment No.	15	16	17	18	19	20	21	22	23	24	25	26	27	28
No. of iterations	2	2	2	2	2	2	2	2	2	2	2	3	3	3

Remark: Quadratic convergence is achieved.

Table I.
Convergence tests of finite elements in Abaqus

Tests	Abaqus finite elements	No. of elements	Applied loads $u_x = u_y = u_z$(mm)	Increment type	No. of disp. Increments	Convergence rate
1	C3D8	1	0.05	Fixed	1	Quadratic
2	C3D8	1	1	Fixed	25	Over linear
3	C3D8	125	0.5	Fixed	25	Quadratic
4	C3D8H	1	1	Fixed	2	Quadratic
5	C3D8H	125	0.5	Fixed	25	Over linear
6	C3D8IH	1	1	Fixed	25	Quadratic
7	C3D20	1	0.05	Fixed	1	Quadratic
8	C3D20H	125	0.05	Fixed	10	Over linear
9	C3D20RH	1	0.05	Fixed	1	Linear
10	C3D6	125	0.5	Fixed	25	Over linear
11	C3D6H	125	0.05	Fixed	25	Over linear
12	C3D4	125	0.5	Fixed	25	Quadratic
13	C3D4H	125	0.05	Fixed	25	Over linear

C3D8	8-node linear brick (hexahedral) B-bar element
C3D8H	8-node hybrid linear brick element with constant pressure
C3D8IH	8-node linear brick, incompatible modes element
C3D20	20-node quadratic brick element
C3D20H	20-node quadratic hybrid brick element with linear pressure
C3D20RH	20-node hybrid quadratic brick element with reduced integration and linear pressure
C3D6	6-node linear triangular prism element
C3D6H	6-node hybrid linear triangular prism element with constant pressure
C3D4	4-node linear tetrahedral element
C3D4H	4-node hybrid linear tetrahedral element with constant pressure

Table II.
Abaqus finite elements

Second material model

Elastic energy from hyperelastic material model

Consistent with the assumption of elastic and thermal isotropy the stored split elastic energy ψ reads, see, e.g. Simo and Hughes (1998):

$$\psi(\mathbf{b},J) = W(J) + \bar{W}(\bar{\mathbf{b}}), \tag{44}$$

with the deviatoric part of elastic left Cauchy-Green tensor, $\bar{\mathbf{b}} := J^{-2/3}\mathbf{F}\mathbf{F}^{\mathrm{T}} \equiv J^{-2/3}\mathbf{b}$, where $W : \mathbb{R}_+ \rightarrow \mathbb{R}_+$. W{0} is a convex function of $J := \det \mathbf{F}$. $W(J)$ and $\bar{W}(\bar{\mathbf{b}})$ are the volumetric and deviatoric parts of ψ, respectively. The following explicit forms are considered:

$$W(J) := \frac{1}{2}\,\kappa\left[\frac{1}{2}(J^2-1) - \ln J\right], \quad \bar{W}(\bar{\mathbf{b}}) := \frac{1}{2}\mu(\mathrm{tr}[\bar{\mathbf{b}}] - 3) \tag{45}$$

where μ and κ are the shear modulus and bulk modulus for linearized strains, respectively.

For the uncoupled elastic energy function equation (44), Kirchhoff stress tensor $\boldsymbol{\tau} = \mathrm{J}\boldsymbol{\sigma}$, is obtained by (Simo and Hughes, 1998):

$$\boldsymbol{\tau} = Jp\cdot\mathbf{1} + \mathbf{S}; \quad p = \frac{\delta W}{\delta J} \tag{46}$$

with $p = (k/2)(1/J)(J^2-1)$ and $\mathbf{S} = \mathrm{dev}[\boldsymbol{\tau}] = \mu\mathrm{dev}[\bar{\mathbf{b}}] = \mu(\bar{\mathbf{b}} - (1/3)\mathrm{tr}[\bar{\mathbf{b}}]\cdot 1)$,

$$\boldsymbol{\tau} = \left[\frac{1}{2}\,\kappa(J^2-1)\mathbf{I} + \mu\left(\bar{\mathbf{b}} - \frac{1}{3}\mathrm{tr}[\bar{\mathbf{b}}]\mathbf{I}\right)\right]. \tag{47}$$

The Cauchy stress tensor reads:

$$\boldsymbol{\sigma}(\mathbf{b},J) = \frac{1}{J}\left[\frac{1}{2}\,\kappa(J^2-1)\mathbf{I} + \mu\left(\bar{\mathbf{b}} - \frac{1}{3}\mathrm{tr}[\bar{\mathbf{b}}]\mathbf{I}\right)\right]. \tag{48}$$

Spatial elasticity tensor

Using Kirchhoff stress tensor equation (47), the spatial elastic tensor $\mathbf{c}$ (Simo, 1998) derived as:

$$\mathbf{c}^{\boldsymbol{\tau}} = J^2\left(\frac{\partial^2 W}{\partial J \partial J}\right)1\otimes 1 + J\frac{\partial W}{\partial J}(1\otimes 1 - 2\mathbb{I}) + \tilde{\mathbf{c}} \tag{49}$$

$$\text{where } \tilde{\mathbf{c}} = 2\bar{\mu}\left[\mathbb{I} - \frac{1}{3}1\otimes 1\right] - \frac{2}{3}\mu[\text{dev}[\bar{\mathbf{b}}]\otimes 1 + 1\otimes\text{dev}[\bar{\mathbf{b}}]], \tag{50}$$

$$\bar{\mu} = \mu\frac{1}{3}\text{tr}[\bar{\mathbf{b}}], \text{ and} \frac{\partial^2 W}{\partial J \partial J} = \frac{k}{2}\left(1 + \frac{1}{J_i^{e2}}\right). \tag{51}$$

Inserting $\partial^2 W/\partial J\partial J$ and $\partial W/\partial J$ in equation (49) yields:

$$\mathbf{c}^{\boldsymbol{\tau}} = J^2\frac{k}{2}\left(1 + \frac{1}{J^2}\right)1\otimes 1 + J\frac{k}{2}\frac{1}{J}(J^2 - 1)(1\otimes 1 - 2\mathbb{I}) + \tilde{\mathbf{c}} \tag{52}$$

$$= kJ^2 1\otimes 1 - k(J^2 - 1)\mathbb{I} + \tilde{\mathbf{c}}. \tag{53}$$

In index notation it reads as:

$$\mathbf{c}_\tau^{abcd} = kJ^2\delta^{ab}\delta^{cd} - k(J^2 - 1)\mathbb{I}^{abcd} + \tilde{\mathbf{c}}^{abcd} \text{ with } \mathbb{I}^{abcd} = \frac{1}{2}(\delta^{ac}\delta^{bd} + \delta^{ad}\delta^{bc}), \tag{54}$$

$$\begin{aligned} \mathrm{c}_\tau^{abcd} = \mathrm{kJ}^2\delta^{ab}\delta^{cd} - \mathrm{k}(\mathrm{J}^2 - 1)\mathbb{I}^{abcd} + 2\bar{\mu}\left[\mathbb{I}^{abcd} - \frac{1}{3}\,\delta^{ab}\delta^{cd}\right] \\ - \frac{2}{3}\mu\left[\text{dev}[\bar{\mathbf{b}}^{-ab}]\delta^{cd} + \delta^{ab}\text{dev}[\bar{\mathbf{b}}^{-cd}]\right] \end{aligned} \tag{55}$$

By inserting $\bar{\mu}$, equation (51), the elastic stiffness yields:

$$\begin{aligned} \mathbf{c}_\tau^{abcd} = kJ^2\delta^{ab}\delta^{cd} - k(J^2 - 1)\mathbb{I}^{abcd} + \frac{2}{3}\mu\text{tr}[\bar{\mathbf{b}}]\left[\mathbb{I}^{abcd} - \frac{1}{3}\,\delta^{ab}\delta^{cd}\right] \\ - \frac{2}{3}\mu\left[\bar{\mathbf{b}}^{ab}\delta^{cd} + \delta^{ab}\overline{b}^{-cd} - \frac{2}{3}\text{tr}[\bar{\mathbf{b}}]^{-ab}\delta^{cd}\right]. \end{aligned} \tag{56}$$

The elastic stiffness associated with Cauchy stress tensor in index notation reads,

$$\mathbf{c}^{abcd} = \mathbf{c}_\tau^{abcd}/J. \tag{57}$$

By using equations (36), (47) and (57) we get the tangent for Abaqus UMAT interface.

Implementation of material model is tested by computation of uniaxial tensile test specimen made up of CuAlNi (Xiangyang *et al.*, 2000). The material data, Poisson's ratio = 0.35 and Young's modulus = 17,200 MPa for the linearized strain is obtained from (Xiangyang *et al.*, 2000). For comutation only the effective part (gauge length 25 mm) of tension specimen is analyzed. The shape of the specimen (flat rectangular cross-section) for numerical validation with the 3D finite element mesh using B-bar linear hexahedral elements (C3D8) and boundary conditions are shown in Figure 4. This model is 25 mm long, 4 mm wide and 1 mm thick. For computation of the uniaxial tension test right face EFHG is fixed in Y direction (as direction 2), points B, D, F and G are fixed in X direction (as direction 1) and points A, C, H and E are fixed in Z direction (as direction 3). A multi-point constrain (MPC) equation is made between face ABCD

and point RP-1 in such a way that surface ABCD will follow the point RP-1. The displacement loads are applied at RP-1 in Y direction (as direction 2). For easy computation of engineering stress-strain date the MPC are made to get the overall reaction force at point RP-1. The spatial FE-discretization was carried out with 176 linear 8-node B-bar hexahedral elements of the type C3D8 in Abaqus.

For this test also quadratic convergence is achieved. Figure 5 shows stress-strain functions obtained from the the implemented material model.

Conclusions

The convergence problem of first and second order B-bar finite elements for finite elasticity – here with Neo-Hookean material – are investigated using Abaqus-UMAT. This interface requires Jaumanm rate of Kirchoff stress tensor for both, rate dependent and rate independent problems. The requested – consistent – tangent is presented in

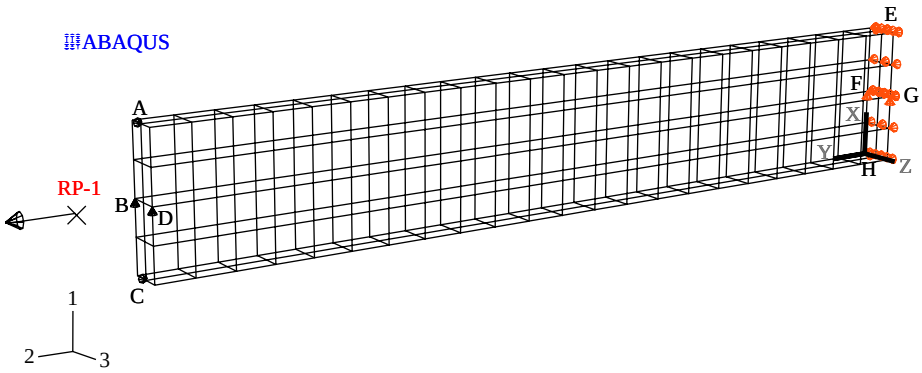

Figure 4.
Geometry and 3D finite element discretization of a PT-tension specimen in reference configuration with boundary condition and displacement-controlled load

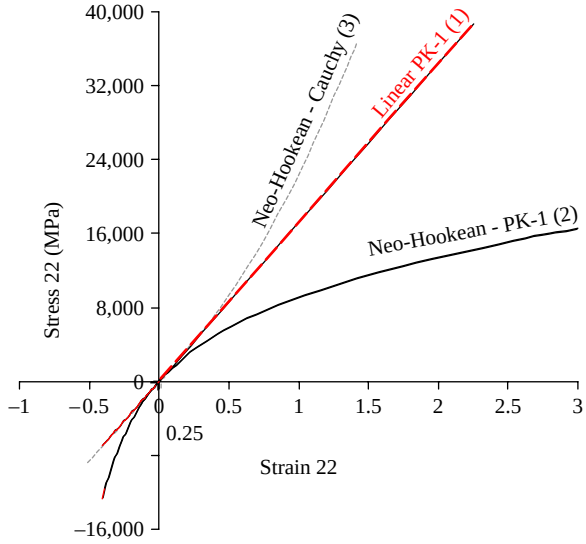

Figure 5.
The curves (1) at linearized strain and (2) at finite strain with Neo-Hookean material hold for engineering stress, F/A_0 - engineering strain, $\Delta \mathbf{l}/\mathbf{l}_0$ relations, and curve (3) represents Cauchy stress, F/A – logarithmic strain, $\ln(\mathbf{l}/\mathbf{l}_0)$ relation

ready-to-use form which is beyond the representation in the Abaqus manuals (Abaqus, n.d.). Furthermore, the Jaumann rate of left Cauchy-Green deformation tensor is used for getting numerical tangent.

In comparing the convergence behaviour for Jaumann rate of Kirchoff stress with analytical and numerical tangent for 14 basic examples using hexahedral, tetrahedral and triangular prism yields the result that only the tangent with Jaumann rate of Kirchoff stress gurantee the quadratic or nearly quadratic convergence.

References

Abaqus (n.d.), *User's Manual, Version 6.4-6.6*, Hibbit, Karlson & Sorensen, Inc., Pawtucket, RI.

Besdo, D., Hohl, C. and Ihlemann J. (2005), "Abaqus implementation and simulation results", in Austrell, P-E. and Kari, L. (Eds), *Constitutive Models for Rubber IV*, Taylor & Francis, London.

de Bore, R. and Schröder, J. (2007), *Tensor Calculus for Engineers with Applications to Continuum and Computational Mechanics*, 1st ed., Springer-Verlag, Berlin.

Miehe, C. (1996), "Non-linear computation of algorithmic (consistent) tangent moduli in large-strain computational inelasticity", *Computer Methods in Applied Mechanics and Engineering*, Vol. 134, pp. 223-40.

Simo, J.C. (1998), "A framework of nite strainelastoplasticity based on maximum plastic dissipation and the multiplicative decomposition: part 1. continuum formulation", *Computer Methods in Applied Mechanics and Engineering*, Vol. 66, pp. 199-219.

Simo, J.C. and Hughes, T.J.R. (1998), *Computational Inelasticity*, Springer, Berlin.

Stein, E. and Sagar, G. (2007), "Theory and finite element computation of cyclic martensitic phase transformation at finite strain", *International Journal for Numerical Methods in Engineering*.

Stein, E. and Zwickert, O. (2007), "Theory and finite element computations of a unified cyclic phase transformation model for monocrystalline materials at small strain", *Computational Mechanics*, Vol. 6, pp. 429-45.

Wriggers, P. (2001), *Nichtlineare Finite-Element-Methoden*, Springer, Berlin.

Xiangyang, Z., Qingping, S. and Shouwen, Y. (2000), "A non-invariant plane model for the interface in cualni single crystal shape memory alloys", *Journal of the Mechanics and Physics of Solids*, Vol. 48, pp. 2163-82.

Corresponding author
Erwin Stein can be contacted at: stein@ibnm.uni-hannover.de

This article has been cited by:

1. J. P. S. Ferreira, M. P. L. Parente, M. Jabareen, R. M. Natal Jorge. 2017. A general framework for the numerical implementation of anisotropic hyperelastic material models including non-local damage. *Biomechanics and Modeling in Mechanobiology* **16**:4, 1119-1140. [Crossref]
2. João Ferreira, Marco Parente, Renato Jorge. 2017. Modeling of soft tissues with damage. *Proceedings of the Institution of Mechanical Engineers, Part L: Journal of Materials: Design and Applications* **231**:1-2, 131-139. [Crossref]
3. M. Genet, L. C. Lee, B. Baillargeon, J. M. Guccione, E. Kuhl. 2016. Modeling Pathologies of Diastolic and Systolic Heart Failure. *Annals of Biomedical Engineering* **44**:1, 112-127. [Crossref]
4. João Ferreira, Marco Parente, Renato Natal. 2015. Fibre Reinforcement in Living Cells: A Preliminary Study of the F-actin Filaments. *Procedia Engineering* **110**, 2-7. [Crossref]
5. Tim Brepols, Ivaylo N. Vladimirov, Stefanie Reese. 2014. Numerical comparison of isotropic hypo- and hyperelastic-based plasticity models with application to industrial forming processes. *International Journal of Plasticity* **63**, 18-48. [Crossref]
6. Tobias Waffenschmidt, César Polindara, Andreas Menzel, Sergio Blanco. 2014. A gradient-enhanced large-deformation continuum damage model for fibre-reinforced materials. *Computer Methods in Applied Mechanics and Engineering* **268**, 801-842. [Crossref]
7. A. Goel, A. Sherafati, M. Negahban, A. Azizinamini, Yenan Wang. 2011. A finite deformation nonlinear thermo-elastic model that mimics plasticity during monotonic loading. *International Journal of Solids and Structures* **48**:20, 2977-2986. [Crossref]
8. Cyprian Suchocki. 2011. A Finite Element Implementation of Knowles Stored-Energy Function: Theory, Coding and Applications. *Archive of Mechanical Engineering* **LVIII**:3. . [Crossref]